Nov 3rd, 12:00 AM

Evaluation of the Flexural Strength of Cold-formed Steel Studs with Embossed Flanges

K. B. Reynolds

S. F. Stephens

Roger A. LaBoube
Missouri University of Science and Technology, laboube@mst.edu

Twentieth International Specialty Conference on Cold-Formed Steel Structures
St. Louis, Missouri, U.S.A., November 3 & 4, 2010

EVALUATION OF THE FLEXURAL STRENGTH OF COLD-FORMED STEEL STUDS WITH EMBOSSED FLANGES

K. B. Reynolds[1], S. F. Stephens[2] and R. A. LaBoube[3]

Abstract

New advances and improvements in the manufacture of cold-formed steel shapes are continually being made. One such advancement in the manufacturing of steel studs is flange embossing, a technique used to facilitate the installation of drywall screws into the stud flange. Currently, embossed flanges are not specifically addressed in the *North American Specification for the Design of Cold-Formed Steel Structural Members* (AISI S100), thereby drawing into question the use of current design equations from being used to calculate member properties for an embossed stud.

A limited experimental investigation was undertaken to determine if light flange embossing affects the nominal flexural strength of cold-formed steel studs. Studs with embossed flanges were tested in bending and their actual flexural strength was determined. This data was then compared with the nominal flexural strength without embossing calculated using AISI S100-07 equations. The findings indicate that light flange embossing does not adversely affect the bending strength of the stud either negatively or positively and therefore, based on the scope of this study, the equations in AISI S100-07 for nominal flexural strength can be applied to lightly embossed studs.

---

[1]Former Graduate Student, Department of Architectural Engineering and Construction Science, Kansas State University

[2]Associate Professor, Department of Architectural Engineering and Construction Science, Kansas State University, Manhattan, Kansas

[3]Distinguished Teaching Professor, Department of Civil, Architectural and Environmental Engineering, Missouri University of Science and Technology, Rolla, Missouri

Introduction

One application of cold-formed steel is as wall studs in light frame and commercial construction. One common use for cold-formed steel studs is curtain walls. According to the AISI S200*, North American Standard for Cold-Formed Steel Framing—General Provisions* (AISI 2007b), a curtain wall is "[a] wall that transfers transverse (out of plane) loads and is limited to a superimposed vertical load, exclusive of sheathing materials, of not more than 100 pounds per foot or a superimposed vertical load of not more than 200 lbs." The studs tested in this investigation are designed for use in curtain walls. These studs are generally sheathed with gypsum or OSB attached with screws, and resist distributed out-of-plane loads applied to the surface of the sheathing. Under this loading, flexural strength is very important, while axial compressive strength is less so. One shape commonly used for steel studs is a C-section. This shape consists of relatively large web with top and bottom flanges, each with a stiffener. Traditionally, the only cold working done to the sheet steel is four bends to form the different elements of the shape, leaving the surface of each of the elements (web, flanges, and stiffeners) smooth along the entire length of the member.

Some manufacturers offer studs with embossed flanges. Embossing is a process where small indentations, often called knurls, are pressed into the flange of the stud as shown in Figure 1. Embossing is not done to enhance the strength of the member, but rather to improve the connection of screws into the flanges. However, as these embossed studs are not currently specifically addressed in AISI S100 for either determination of member properties or nominal strength. This brings into question the use of the AISI S100 design equations to determine the capacities of this stud configuration.

Purpose of Investigation

The purpose of this investigation was to determine whether flange embossing affects the member properties of cold-formed studs. Specifically, studs with embossed flanges were tested in bending in an effort to determine if embossed flanges adversely affect the nominal flexural strength of a curtain wall stud in a fully braced condition. The flexural strengths determined by testing were compared to the calculated nominal flexural strength assuming the embossments were not present to determine if the strength is altered by the presence of the embossments. Two common depths of cold-formed steel studs, 3.625 inches (92 mm) and 6 inches (152 mm), both 18 mil minimum thicknesses and with embossed flanges, were investigated. This material thickness was selected because the embossing was more pronounced than it would have been on a thicker section, so this should be the most severe situation.

Experimental Investigation

Material Properties and Cross-Sectional Geometry

The cold-formed steel studs used in this investigation were donated by Telling Industries of Cambridge, OH. Two sizes were tested; 362S125-18, and 600125-18. All studs had 1.5-in (38.1 mm) web punchouts spaced at 24" OC (610 mm), starting 12-in (305 mm) from the end of the stud.

To determine the actual mechanical properties of the steel, coupons were cut from the center of the webs to avoid a potential increase in F_y due to cold work of forming. Coupons were milled to width and subjected to an ASTM A370 standard tensile test. The results of the tensile test based on the measured uncoated cross sectional area are shown in Table 1.

Additionally, the full cross sections were carefully measured to determine the dimensions, including radii of bends and angles of the flange stiffeners. The dimensions of the embossments (Figure 2) were also measured, and are listed in Table 2.

The measured dimensions were then input into RSG Software's CFS program, Version 6.0.2, (RSG 2009), to compute the section properties and the nominal flexural strength of the sections using provisions from AISI S100 (AISI 2007a).

Test Specimens

Test specimens were constructed of two 8'-0" (2.44 m) long C-studs assembled in an open box configuration with their flanges toward the center of the specimen (Figure 3). A box section was used to provide a more laterally stable specimen than a single stud. The test was designed so that the failure mode would be flexure. The width of the specimen was 5.5 inches (139.7 mm).

All specimens were assembled with #8 x ¾-in (19 mm) self-drilling screws. ¾-in (19 mm) wide cold-rolled channel (CRC) were used to form the box-shaped test specimen. The channels were placed at 12-in (305 mm) on center along both top and bottom flanges (Figure 4). This spacing was chosen to represent the way gypsum board is often attached in the field, using screws at a maximum of 12-in (305 mm) on both sides of the stud.

To prevent web crippling, each specimen was reinforced with web stiffeners at the end supports and points of load application. Segments of cold-formed studs, with length equal to the depth of the specimen and oriented perpendicular to the specimen, were used as web stiffeners, which were attached to the specimens with five No. 8 screws. For the first three specimens tested of each size (specimens 3A, 3B, 3C, 6A, 6B, and 6D), the stiffeners were made from the

same size stud that was being tested. In the second set of tests, all web stiffeners were cut from 3.625-in (92 mm) studs, and stiffeners at the point of load application were also extended approximately ⅛" (3.2 mm) above the top flange, to provide load transfer directly to the web thus avoiding buckling of the flange from local stresses at the bearing plates. This change was made because in the first set of three tests it was discovered that loading directly on the flanges may have been causing a concentration of stresses leading to premature flange buckling. For this stiffener configuration, six No. 8 screws were used per stiffener to ensure full load transfer from the stiffener to the specimen web. All specimens were also braced against torsional buckling at the end reactions with dimensional 2x wood blocking (3"x5.5"x1.5" (76x140x38 mm) for the 3.625-in (92 mm) specimens and 5.5"x5.5"x1.5" (140x140x38 mm) for the 6-in (152 mm) specimens).

Test Setup

Specimens were tested in a simple span condition with two concentrated loads located at third points of the beam, 2'-8" (813 mm) (Figure 4,5,6) from beam ends creating a constant moment region with zero shear in the central span between the loads. Third points were selected for loading because they provided a constant moment region and provided balanced loading. Loads were applied to the specimens at the location of the web stiffeners through 4-in (102 mm) wide steel plates. Bearing plates at the end reactions were also 4-in (102 mm) wide, and one support was a sliding bearing plate to allow for longitudinal movement of the specimen.

To prevent lateral displacements of the test specimens, four large, hot rolled steel brackets were arranged with wooden shims to restrain the specimen laterally while still allowing it to deflect vertically. These braces were located at 8 inches from load points (Figure 6). One 3.625-in (92 mm) specimen (specimen 3E) 6'-6" (1.98 m) in length was also tested.

Test Procedure

Tests were conducted using an MTS Flextest GT unit, with a 22-kip actuator and load cell. Time, load, and stroke displacement were measured and recorded through a MultiPupose TestWare (MPT) program written to control the actuator. Additionally, a linear variable differential transformer (LVDT) was used at midspan to measure deflection. Deflection data was also continually recorded through the MPT software.

The actuator was run in a displacement-controlled manner at a rate of 0.1 inch (2.5 mm) per minute. Each specimen was loaded until it would take no more load.

Test Results and Evaluation of Data

A total of ten specimens were tested (five from 3.625-in (92 mm) studs and five from 6-in (152 mm) studs) and were loaded until local or distortional buckling reduced the resistance to the point that they would not take any more load. All of the specimens failed in a similar manner; by flange local buckling. In some cases, after the flange local buckling was observed, buckling of the web below the flange buckle was noted (Figure 7). After each specimen was tested, the tested flexural strength was computed for the specimen as a whole. The nominal flexural strength was also calculated using the CFS program based on AISI S100-07. These two values were then compared to determine the applicability of the AISI S100 flexural equations for embossed-flanged studs.

In 60% of the tests conducted, failure occurred at the punchouts (Figure 4). The punchouts were considered in the calculation of the nominal flexural strength. Failure by buckling at these locations is as expected since the section properties for bending are most critical at the punchouts.

Results for the 3.625-in (92 mm) Specimens

Table 3 summarizes the results obtained for the 3.625-in (92 mm) specimens. The first column shows the test yield stress, F_y found in the tensile tests. The next columns show the configuration of the test, referencing the dimensions shown in Figure 5. The total test load, P_t, is the total read from the load cell plus the weight of the bearing plates and spreader beam, and is the total of both point loads applied. The displacement shown was recorded by the load cell, and represents the displacement at the point of load application.

Figure 8 shows a graph of the force and displacement of a representative test of the 3.625-in (92 mm) test specimens. The graph starts at 100 pounds (445N) due to the weight of the plates and spreader beam on the specimen prior to the beginning of the test. The two peaks on this graph represent the two different studs that comprise the specimen buckling at slightly different loads. The predicted displacement is also displayed calculated using the section properties from CFS. As can be seen, once the predicted displacement line is shifted to exclude initial deflection, the measured displacements correlated with the predicted.

Table 4 shows the values of the maximum load resisted by each specimen based on the test results. From this, the tested moment capacity was calculated for a single stud. The computed nominal moment capacity, M_n, is also listed in table 4. Using the CFS software, checking both distortional and elastic local buckling, it was found that the governing limit state for this size stud was elastic local buckling based on the effective section modulus. Finally, the ratio of the

bending moment based on the test load to the calculated nominal flexural strength is shown.

Results for the 6-in (152 mm) Specimens

Table 5 summarizes the results of the bending tests on the 6-in (152 mm) specimens. The yield stress found in the coupon test is shown. The loading configuration data, again referencing Figure 5, is in the next three columns. The maximum load shown in the table is the total load applied by the load cell including the weight of the bearing plates and spreader beam to the overall specimen. The displacement recorded in the table represents the displacements at points of load application.

The graph shown in Figure 9 is a representative sample force-displacement graph for one of the 6-in (152mm) specimens. Again, the graph starts at 100 pounds (445 N) due to the spreader beams and load plates. This graph has a single peak, indicating that both members flange buckled simultaneously. This graph also shows the predicted displacement. For this specimen, once the initial deflection is accounted for the actual deflections again correlated with the predicted.

Table 6 shows the maximum load applied to each of the 6-in (152 mm) specimens. This was used to calculate the tested bending capacity of a single stud, shown in the next column. The nominal flexural strength as calculated per AISI S100 is also shown. For the 6-in (152 mm) studs, it was found that the distortional buckling calculated by the direct strength method was the governing limit state. The ratio of the bending moment based on the test load to calculated nominal flexural strength is presented in Table 6, as well.

Conclusions

For both stud sizes, the data was examined to determine if the presence of flange embossing resulted in a reduction in the flexural capacity for the stud below the nominal flexural strength computed by the provisions of the AISI S100-07.

For the 3.625-in (92 mm) studs, all tested moment capacities fall within 5% of the calculated value of M_n. The mean value for all 5 tests is 1.044 with a coefficient of variation of 0.0516. Comparing these results to the test data base used for the development of the design equations, these results would fall within the scatter of the previous testing programs.

For the 6-in (152mm) studs, once again, the tested moment capacities all surpass the computed values for M_n. The mean ratio of tested moment capacity to nominal flexural strength was 1.0361, with a coefficient of variation of 0.0274. Again, this data fits within the scatter of the previous test results. As an

example of this, on page 75 of the Direct Strength Method Design Guide (AISI 2006), Table 5 shows for 185 tested C-sections, the mean is 1.10, but the V_p is 0.11. This V_p is much larger than was obtained in this study, suggesting that this data would indeed fit into the scatter of the previous tests.

Based on the findings of this study, embossing of the flanges on the specimens tested did not adversely affect the flexural capacity of the studs. Therefore, it is concluded that the AISI S100 provisions may be appropriate for the determination of both section properties and nominal flexural strength.

The authors wish to thank Telling Industries, for their donation of the materials used in this testing program.

References

AISI (2006), *Direct Strength Method Design Guide,* American Iron and Steel Institute, Washington D.C.

AISI-S100 (2007a), *North American Specification for the Design of Cold-Formed Steel Structural Members,* American Iron and Steel Institute, Washington D.C.

AISI-S200 (2007b), *North American Standard for Cold-Formed Steel Framing—General Provisions* American Iron and Steel Institute, Washington D.C.

ASTM Subcommittee A01.13. (2008). *ASTM A370 - 09 Standard Test Methods and Definitions for Mechanical Testing of Steel Products.* ASTM International, West Conshohocken, PA

RSG Software. (2009) *CFS Version 6.0.2.* Lee's Summit, MO

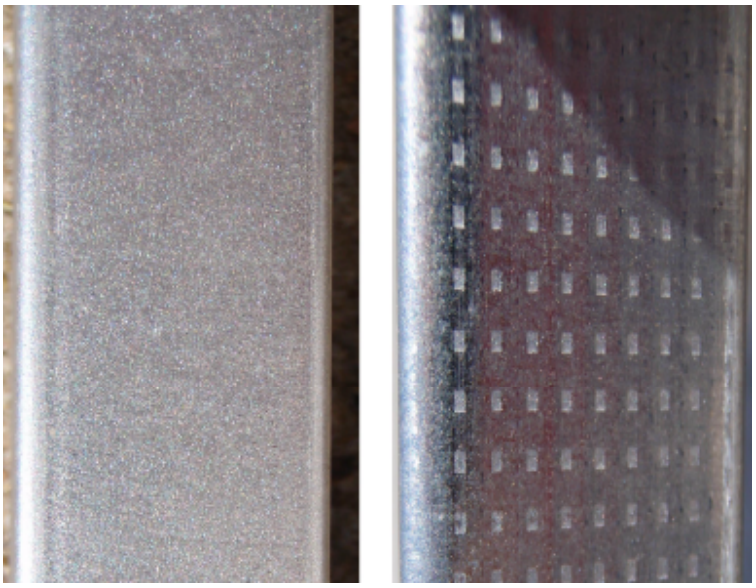

Figure 1: Flange of a smooth stud and an embossed flange.

Table 2: Tensile Test Results

Specimen	t (in.)	w(in.)	F_y (ksi)	F_u(ksi)	Percent Elongation
3A	0.0170	0.95	50.5	58.4	9.59
3B	0.0168	0.95	51.5	59.6	9.58
6A	0.0188	0.95	51.0	60.0	9.56
6B	0.0185	0.95	52.0	61.7	9.56
For SI: 1 in. = 25.4 mm, 1 ksi = 6.8 MPa					

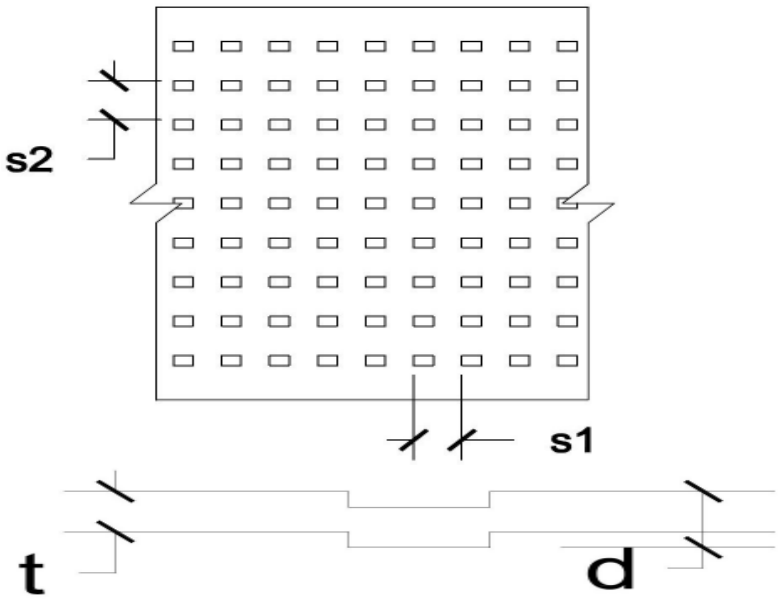

Figure 2: Dimensions for embossments.

Table 2: Embossment dimensions

Section	t	d	s1	s2
362S125-18	0.0171	0.019	0.116	0.116
600S125-18	0.0187	0.0211	0.116	0.116
Note:	All dimensions in inches (1 in = 25.4 mm).			

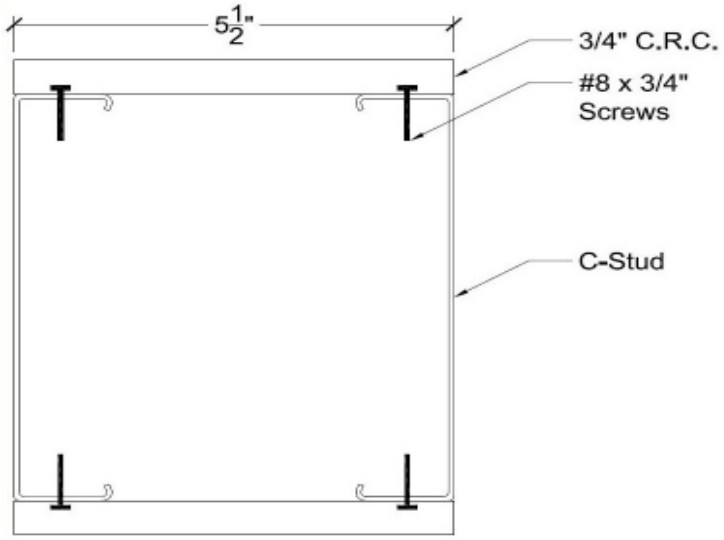

Figure 3: Typical test specimen cross section.

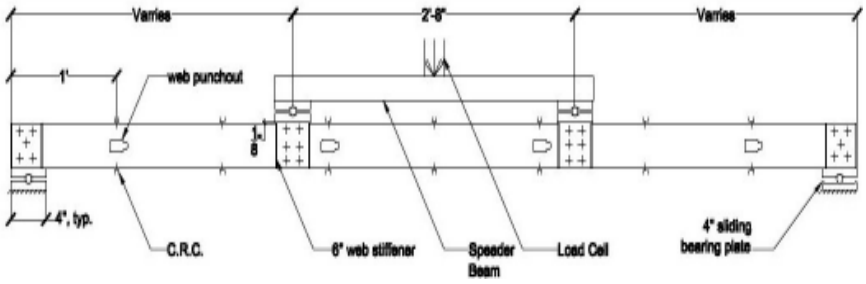

Figure 4: Test specimen (3.625-in (92 mm)) showing extended web stiffeners.

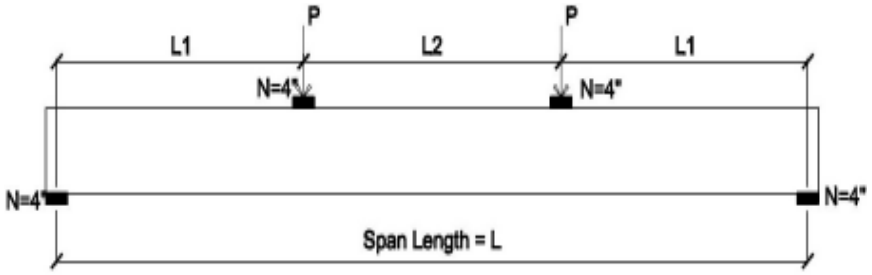

Figure 5: Typical loading configuration.

Figure 6: 6-inch (152 mm) test specimen set-up.

Figure 7: Typical flange buckling failure shown on a 6 in. (152 mm) specimen.

Table 3: Configuration and test loads for 3.625-in (92 mm) specimens.

Specimen	F_y (ksi)	Span L	Loading Dims L1	Loading Dims L2	P_t (lbs.)	Disp. (in.)
3 A	51	7'-8"	2'-8"	2'-8"	396.88	0.439
3 B	51	7'-8"	2'-8"	2'-8"	396.71	0.439
3 C	51	7'-8"	2'-8"	2'-8"	404.27	0.495
3 D	51	7'-8"	2'-8"	2'-8"	388.16	0.459
3 E*	51	6'-6"	1'-11"	2'-8"	494.61	0.411

Note:
P_t = Total test load
L1 and L2 (Refer to Figure 5)
*-This sample was shortened due to shipping damage at its ends.
For SI: 1 ksi = 6.8 MPa, 1 ft = 0.305 m, 1 lb = 4.45 N, 1 in = 25.4 mm

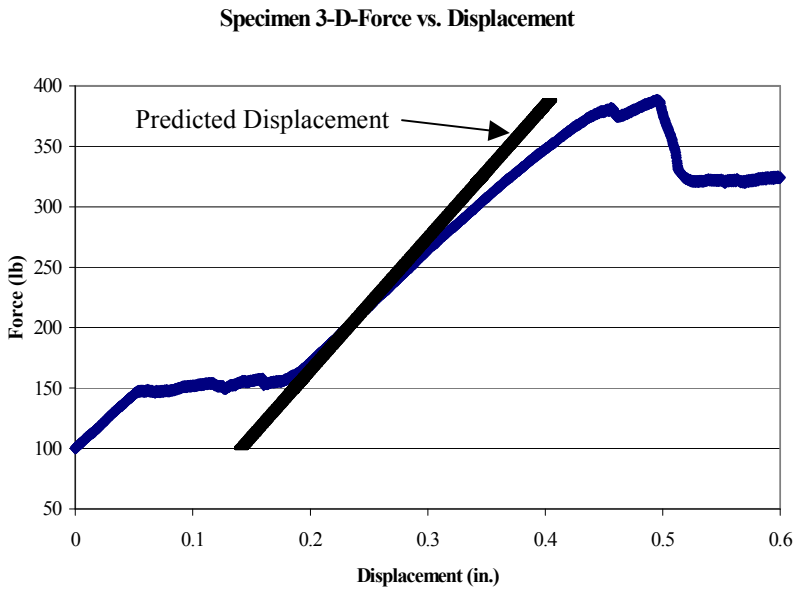

Figure 8: Force-Displacement graph for specimen 3D.

For SI: 1 lb. = 4.45 N, 1 in. = 25.4 mm

Table 4: Nominal flexural capacity comparison, 3.625-in. (92mm) specimen.

Specimen	P_t (lbs.)	M_t (k-in.)	M_n (k-in.)	M_t/M_n
3 A	396.88	6.350	5.951	1.067
3 B	396.71	6.347	5.951	1.067
3 C	404.27	6.468	5.951	1.087
3 D	388.16	6.210	5.951	1.044
3 E	494.61	5.688	5.951	0.956

Note: P_t = Total test load
M_t = Test moment
M_n = Computed nominal flexural strength
For SI: 1 lb.=4.45 N, 1 k-in.=113 Nm

Table 5: Configuration and test loading for 6-in (152 mm) specimens.

Specimen	F_y (ksi)	Span L	Loading Dims L1	Loading Dims L2	P_t (lbs.)	Disp. (in.)
6 A	51.5	7'-8"	2'-8"	2'-8"	706.39	0.444
6 B	51.5	7'-8"	2'-8"	2'-8"	716.09	0.442
6 C	51.5	7'-8"	2'-8"	2'-8"	702.12	0.415
6 D	51.5	7'-8"	2'-8"	2'-8"	745.71	0.396
6 E	51.5	7'-8"	2'-8"	2'-8"	736.83	0.363
Note:	P_t = Total test load L1 and L2 (Refer to Figure 5) For SI: 1 ksi=6.8 MPa, 1 ft = 0.305 m, 1 lb = 4.45 N, 1 in.=25.4 mm					

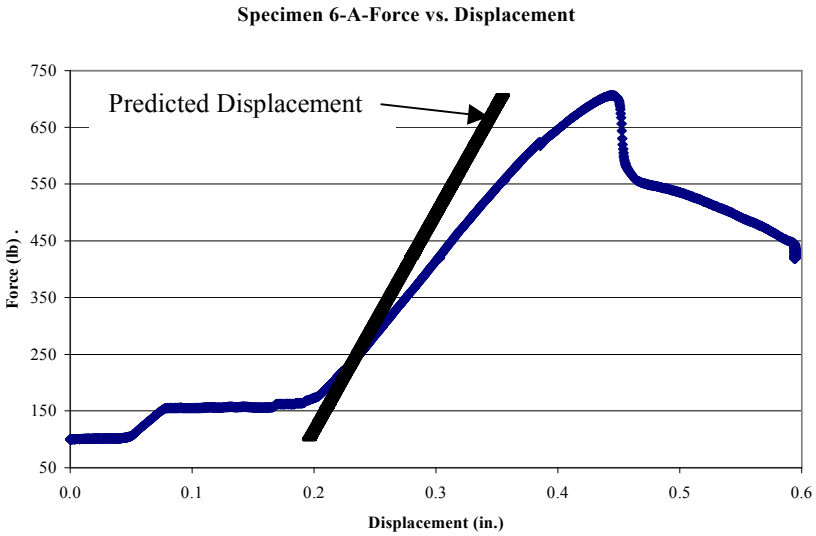

Figure 9: Force-Displacement graph for specimen 6A.

For SI: 1 in=25.4mm, 1 lb =4.45 N

Table 6: Nominal flexural capacity comparison, 6" (152 mm) specimens.

Specimen	P_t (lbs.)	M_t (k-in.)	M_n (k-in.)	M_t/M_n
6 A	706.39	11.302	11.141	1.015
6 B	716.09	11.457	11.141	1.028
6 C	702.12	11.234	11.141	1.008
6 D	745.71	11.931	11.141	1.071
6 E	736.83	11.789	11.141	1.058

Note: P_t = Total test load
M_t = Test moment
M_n = Computed nominal flexural strength
For SI: 1 ksi=6.8 MPa, 1 ft.=0.305 m, 1 lb.=4.45 N, 1 in.=25.4 mm